International Journal of Computer Information Systems and Industrial Management Applications
ISSN 2150-7988 Volume 18 (2026) pp. 1-9

https://doi.org/10.70917/ijcisim-2026-3597
Article

Spatiotemporal Evolution Analysis of Social Media Tourism Hotspots Based on Pulse-Coupled Neural Network and Memristor Cross Array

Qian Zhang [1,2,*] and Zhuoran Zhang [1]

[1] Martin de tours School of Management and Economics, Assumption University, Bangkok, 10540, Thailand
[2] School of Economics and management, Jiaozuo Normal College, Jiaozuo, Henan, 454000, China
* Correspondence author: wairey523@163.com

Abstract: In the spatiotemporal evolution of social media tourism hotspots, feature aliasing leads to computational bottlenecks and low analysis efficiency. Therefore, this study investigates spatiotemporal evolution analysis of social media tourism hotspots based on pulse-coupled neural networks and memristor cross arrays. A hierarchical memristor cross array computational architecture is constructed to adapt to four-dimensional spatiotemporal tourism data and achieve in-situ parallel computation. The dynamic model of the pulse-coupled neural network is reconstructed, and nested coupling operations are introduced to complete pulse coding and unsupervised extraction of multimodal tourism features from social media. Combined with spatial correlation analysis and temporal inference algorithms, tourism hotspot identification, heat quantification, and spatiotemporal evolution law analysis are completed. Experiments show that the research method achieves a spatiotemporal evolution path matching accuracy of 0.975 under a 24-hour daily observation window, and achieves a high-stability classification effect with single-class recognition accuracy exceeding 95% for four types of cultural tourism scenarios. Under a 2048-dimensional high-dimensional feature input scenario, the inference latency is compressed to 18.7ms, and the computation speedup ratio reaches up to 8.7 times, improving the efficiency of spatiotemporal evolution analysis of social media tourism hotspots.

Keywords: Pulse-Coupled Neural Network; Memristor Cross Array; Social Media Tourism Hotspots; Spatiotemporal Evolution; Multimodal Feature Extraction

1. Introduction

As social media becomes an important data source for perceiving tourists' spatiotemporal behavior and tourism flow aggregation characteristics, tourism hotspot detection and spatiotemporal evolution analysis based on geotagged user-generated content (UGC) has gradually become a research hotspot in the fields of tourism geographic information and urban intelligent monitoring.

Foka et al. [1] applied hotspot analysis and prediction methods to mobile network communication scenarios, identifying areas with concentrated service loads through statistical modeling. However, this method relies on high-dimensional computation using centralized processors, resulting in low efficiency under large-scale spatiotemporal data. Yujuan et al. [2] constructed interest hotspot maps using social network check-in data and conducted optimal path recommendations, employing kernel density estimation or sliding window density statistics for grid-by-grid calculation on a general platform. However, this method requires high floating-point operations to maintain the index, leading to high latency under city-level spatiotemporal tensors. Liu et al. [3] conducted hotspot identification and spatial regression analysis of endemic disease health losses at the county level, solving the weight matrix cyclically cell-by-cell based on global or local spatial autocorrelation indices. However, matrix operations become increasingly time-consuming as the grid size or time span increases. Dunkel et al. [4] automatically generated thematic maps based on geographic social media data using a generative diffusion model, completing research related to hotspot perception. However, this method relies on floating-point tensor propagation in convolutional networks, resulting in high resource consumption and difficulty in meeting near real-time requirements.

To this end, this paper proposes a spatiotemporal evolution analysis method for social media tourism hotspots based on pulse-coupled neural network and memristor cross array, aiming to achieve efficient and low-power perception and analysis of the spatiotemporal evolution process of tourism hotspots.

2. Constructing a Memristor Cross Array Computational Architecture Adapted to Tourism Spatiotemporal Data

Social media tourism spatiotemporal data is four-dimensional multimodal data containing space, time, content, and popularity. The spatial dimension covers the latitude and longitude of scenic spots, administrative divisions, and geographic grid information; the time dimension includes posting timestamps, time periods, seasons, and holiday tags; the content dimension includes text sentiment, travel tags, and keyword vectors; and the popularity dimension includes quantified data of likes, reposts, and comments. This data has three major characteristics: sparsity, strong spatiotemporal correlation, and sudden fluctuations [5].

To adapt to the characteristics, the memristor cross array needs to meet three core requirements: hierarchical storage, in-situ parallel operation, and pulse-compatible read/write. This paper cleans and normalizes the UGC data, completes the unification of dimensions, and the standardized data field composition is shown in Table 1.

Table 1. Standardized Social Media Tourism Spatiotemporal Data Field Table

Data dimension	Core fields	Data type	Normalized interval
Spatial dimension	Longitude, latitude, and geographic grid number	Floating point type, integer type	[0,1]
Time dimension	Timestamp, season code, holiday weight	Integer, floating point type	[0,1]
Content dimension	Emotion value, game type label, feature vector	Floating point type, vector type	[-1,1]
Heat dimension	Like count, forward count, comment count	Integer	[0,1] (logarithmic normalization)

Two-dimensional memristor cross arrays cannot distinguish multi-dimensional data attributes, which easily leads to feature aliasing. This paper designs a four-layer hierarchical memristor cross array, corresponding to the spatial layer, time layer, content layer, and heat layer, respectively. Vertically coupled memristors are set between layers to achieve feature fusion.

The conductance of memristor units is jointly regulated by charge migration and interface barrier. Considering the charge accumulation decay effect, its dynamic conductance characteristics can be expressed by formula (1):

$$G(t) = G_{min} + \left(G_{max} - G_{min}\right) \cdot \sigma\left(\oint_{\Omega} I(\tau) \cdot \varphi(\tau) d\tau\right) \cdot \exp\left(-\int_0^t \lambda(x) dx\right) \tag{1}$$

In formula (1), $G(t)$ is the real-time conductance state of the unit; G_{max}, G_{min} are the upper and lower boundary constraints of the device conductance; σ is the nonlinear activation operator of charge response; Ω is the charge integration domain; $I(\tau)$ is the time-series driving current; $\varphi(\tau)$ is the charge migration correction function; $\lambda(x)$ is the conductance decay kernel function, which characterizes the charge leakage characteristics of the device.

This paper embeds the normalized four-dimensional tourism data into the corresponding layer memristor conductance matrix through voltage mapping, realizing in-situ co-storage of data and parameters, and avoiding data scheduling loss between storage and computation. The memristor cross array relies on Kirchhoff's current law to realize parallel matrix operation. Considering the array parasitic resistance coupling interference, the corrected matrix mapping operation is shown in formula (2):

$$I_{out} = \left(V_{in} \cdot G_{blk}\right) \otimes \Phi_{para} + \nabla\left(G_{blk}\right) \tag{2}$$

In formula (2), V_{in} is the input feature voltage vector; G_{blk} is the layered array block conductance weight matrix; Φ_{para} is the array parasitic parameter correction vector; ∇ is the array edge gradient compensation operator to suppress the calculation deviation of the boundary unit.

To address the imbalance between the dimensional differences and correlations of four-dimensional spatiotemporal features, this paper constructs an adaptive weighted fusion model with cross-coupling constraints. The fused feature vector can be expressed by formula (3):

$$F_{agg} = H\left(\alpha F_{sp} + \beta F_{tm} + \gamma F_{cnt} + \delta F_{pop}, \Xi_{cross}\right) \tag{3}$$

In formula (3), F_{sp} , F_{tm} , F_{cnt} , F_{pop} are the original feature vectors of the spatial, temporal, content, and popularity dimensions, respectively; α , β , γ , δ are the adaptive weight coefficients, satisfying the convex combination constraint conditions; Ξ_{cross} is the inter-dimensional correlation coupling matrix; H is the normalized fusion operator with coupling constraints, realizing the enhancement of nonlinear correlation of features.

This chapter completes the construction of a hierarchical memristor cross array adapted to tourism spatiotemporal data. The hierarchical topology and coupled fusion operator solve the problem of feature aliasing in multimodal data. Relying on in-situ computation, sparse masking, and gradient compensation mechanisms, the computational cost is reduced, providing a low-latency, high-parallelism, and low-bias hardware computing foundation for subsequent spiking neural network feature extraction.

3. Training a Pulse-coupled Neural Network for Social Media Feature Extraction

The basic PCNN consists of a feed, a link, and a pulse generation domain, and has the ability to extract unsupervised synchronous pulses, but it has the defects of single input dimension, fixed parameters, and poor multimodal adaptation. This paper makes three modifications to the characteristics of tourism UGC: adding a four-dimensional parallel input path, replacing fixed parameters with memristor-guided synapses, and constructing a dynamic threshold for heat correlation. The modified model structure is shown in Figure 1.

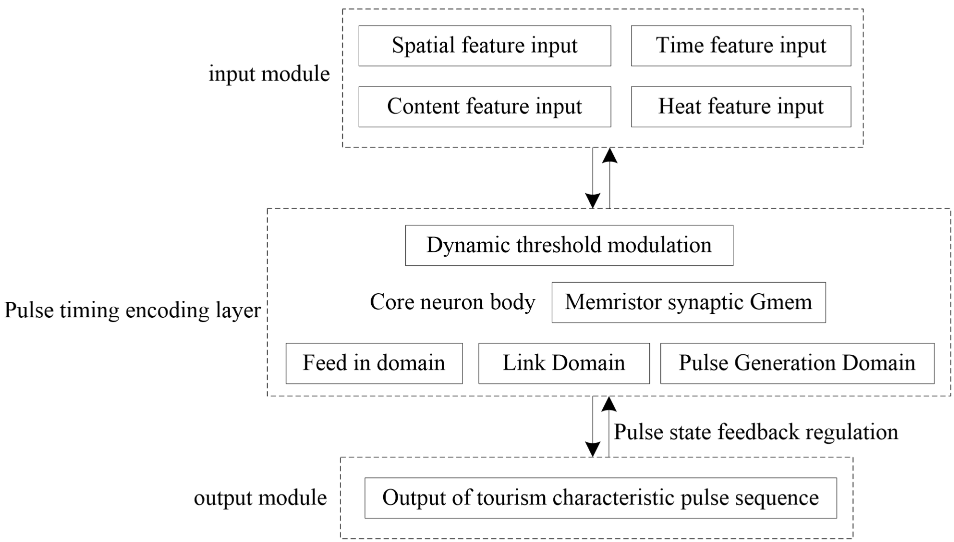

Figure 1. Schematic diagram of the improved PCNN model structure

The continuous aggregation features output by the memristor array cannot directly drive spiking neurons and need to be mapped to discrete pulse sequences [6] through nonlinear temporal coding. This paper adopts an amplitude-temporal composite coding mechanism, combined with feature saliency weights to complete the pulse timing mapping. The coding mapping relationship is shown in formula (4):

$$\tau_k = T\left(F_{agg}[k], \omega_{sig}\right) = T_{max} \cdot \left(1 - N\left(F_{agg}[k] \otimes \omega_{sig}\right)\right) \tag{4}$$

In formula (4), τ_k is the pulse firing time sequence position corresponding to the k dimension feature; T is the temporal coding mapping operator; ω_{sig} is the feature saliency weight vector; N is the global adaptive normalization operator; T_{max} is the coding temporal window boundary.

Based on the coding temporal position, a binary discrete pulse state sequence is generated, and a temporal neighborhood inhibition constraint is introduced. The pulse state generation rule is shown in formula (5):

$$s_k(t)=\begin{cases}U\left(\tau_k-t\right)\cdot M\left(\Gamma_{neigh}[k]\right), & t=\tau_k\\ 0, & t\neq\tau_k\end{cases} \tag{5}$$

In formula (5), $s_k(t)$ is the pulse activation state of neuron k at time t ; U is the step constraint operator; $\Gamma_{neigh}[k]$ is the neuron neighborhood pulse association vector; M is the neighborhood inhibition modulation operator to avoid excessive synchronous activation of neurons at the same time [7].

This paper reconstructs the three-layer coupled dynamic system of neurons, introduces temporal recursive decay, lateral correlation propagation, and threshold dynamic modulation nested operations, and constructs a fully coupled neuron model. The evolution law of the feed signal with recursive memory term can be expressed by formula (6):

$$u_k(t)=A_f\left(u_k(t-1)\right)+\sum_{j\in\Theta_k} w_{kj}\cdot s_j(t-1)+B\left(F_{agg}[k],u_k(t-1)\right) \tag{6}$$

In formula (6), $u_k(t)$ is the feed activation signal of neuron k at t time; A_f is the recursive attenuation operator for the feed signal; Θ_k is the set of neighboring neurons of neuron k ; w_{kj} is the memristor synaptic weight between neurons; B is the feature-state cross-coupling operator, which associates external input with historical activation state.

Considering the bidirectional conduction characteristics of lateral neuron pulses, the evolution of the link domain association signal is shown in Equation (7):

$$v_k(t)=A_l\left(v_k(t-1)\right)+\sum_{j\in\Theta_k} m_{kj}\cdot\left(s_j(t-1)-s_k(t-1)\right)\cdot C\left(|\,\tau_j-\tau_k\,|\right) \tag{7}$$

In Equation (7), $v_k(t)$ is the lateral link signal of neuron k at time t ; A_l is the link signal temporal attenuation operator; m_{kj} is the lateral coupling conduction coefficient; C is the temporal difference modulation kernel function, which characterizes the constraint effect of pulse temporal difference on lateral association.

The dynamic threshold and pulse generation judgment rule of integrating historical activation memory and lateral association feedback are shown in formula (8):

$$\begin{cases}\theta_k(t)=A_\theta\left(\theta_k(t-1)\right)+D\left(s_k(t),v_k(t)\right)\\ s_k(t)=h\left(u_k(t)\cdot\left(1+\mu\cdot v_k(t)\right)-\theta_k(t)\right)\end{cases} \tag{8}$$

In formula (8), $\theta_k(t)$ is the dynamic activation threshold of the neuron; A_θ is the threshold decay memory operator; D is the pulse feedback threshold correction function; μ is the lateral link strength regulation coefficient; h is the activation judgment step operator, which outputs the final pulse state of the neuron.

Relying on the in-situ parallel computing capability of the memristor array, an unsupervised loss function based on pulse synchronization topological similarity is constructed, and a cross-neuron association penalty term is introduced to suppress oversynchronization [8]. The loss function can be expressed by formula (9):

$$L_{total}=-\frac{1}{|\,\Theta\,|^2}\sum_k\sum_j S\left(s_k,s_j\right)\cdot K\left(|\,\tau_k-\tau_j\,|\right)+R\left(W_{syn}\right) \tag{9}$$

In formula (9), $|\,\Theta\,|$ is the global neuron set cardinality; S is the pulse synchronization overlap operator; K is the temporal distance decay kernel; R is the synaptic weight regularization penalty term, which constrains the divergence of weights.

Based on the backpropagation chain rule, the in-situ weight gradient is derived, and the parameter update is achieved through continuous modulation of the memristor conductance. The weight-conductance coupling update rule is shown in formula (10):

$$\Delta w_{kj} = -\eta \cdot \frac{\partial L_{total}}{\partial w_{kj}}, G_{new} = F\left(G_{old}, \Delta w_{kj}, \nabla G_{dev}\right) \tag{10}$$

In formula (10), η is the global learning rate operator; Δw_{kj} is the synaptic weight gradient update amount; G_{old} and G_{new} are the conductance state of the memristor unit before and after the update; ∇G_{dev} is the non-ideal conductance deviation gradient of the device; F is the conductance-weight nonlinear mapping function considering device deviation.

The model adopts an adaptive batch scheduling training strategy. The initial learning rate is dynamically initialized according to the weight distribution. The iteration is terminated when the loss fluctuation is less than the threshold. The entire process relies on the memristor array to complete the gradient calculation and parameter update in situ without external data transfer [9], which greatly reduces the training computing power loss and outputs a high-discrimination tourism attribute pulse feature sequence, providing core support for subsequent hotspot spatiotemporal evolution analysis.

4. Realize the Spatiotemporal Evolution Analysis of Social Media Tourism Hotspots

Based on the global pulse feature sequence output by PCNN, this paper constructs the spatiotemporal coupled heat index (STHI), integrates geographic grid pulse density, social interaction correlation, and temporal pulse persistence to complete the regional heat quantification, introduces spatial neighborhood coupling and temporal decay nested operation to construct a dimensionless heat measurement, and the grid unit and time analysis scale continue the previous settings. The regional comprehensive heat index is generated by coupling the pulse spatial distribution term, social propagation weight term, and temporal persistence term, and the quantification formula is shown in (11):

$$Q_{st} = W_{sp} \otimes P\left(S_{grid}, \Xi_{sp}\right) + W_{tm} \otimes O\left(S_{seq}, \Phi_{tm}\right) + W_{soc} \otimes \varepsilon\left(A_{usr}, \Psi_{soc}\right) \tag{11}$$

In formula (11), Q_{st} is the spatiotemporal coupling heat index of geographic grid unit; W_{sp} , W_{tm} , W_{soc} are the weight operators of spatial, temporal and social dimensions respectively, satisfying the convex combination constraint; P is the grid pulse density distribution function; Ξ_{sp} is the spatial correlation matrix; O is the temporal pulse duration function; Φ_{tm} is the temporal decay kernel; ε is the social interaction energy operator; A_{usr} is the user behavior feature; Ψ_{soc} is the propagation correlation matrix.

Based on the distribution interval of Q_{st} , tourism hotspots are divided into five levels, and the classification criteria are shown in Table 2.

Table 2. Classification of the Spatiotemporal Heat Index of Tourism Hotspots

Hotspot Level	STHI value range	Hotspot type	Regional feature description
Grade I	[0,0.2)	Cold spots in tourism	No social check-in data, no customer flow aggregation
Level II	[0.2,0.4)	Potential hotspots	A small amount of social exposure, initial gathering of customer flow
Grade III	[0.4,0.6)	Regular hot topics	Stable social communication, daily customer flow gathering
Grade IV	[0.6,0.8)	Hot spot with high fever	Widely spread in the region, with peak passenger flow
Grade V	[0.8,1.0]	Explosive hotspots	Viral social spread, excessive passenger flow gathering

Based on the geographic grid mapping relationship of the memristor spatial layer array, combined with the spatial dimension pulse features output by PCNN, the global spatial autocorrelation and local correlation decomposition algorithm is used to mine the hot spot spatial evolution law, quantify the overall regional agglomeration trend and local heterogeneous features, identify high-value agglomeration, low-value agglomeration, and spatial abnormal units, and generate a regional hot spot spatial agglomeration distribution map.

Based on the embedded temporal coding attributes of PCNN pulse sequences, the pulse firing frequency distribution at different time granularities is statistically analyzed. Three types of temporal evolution components—intraday fluctuations, weekly cycles, and seasonal trends—are decomposed. The modulating effect of the external environment on heat fluctuations is quantified by combining holiday and climate weights, outputting refined temporal evolution patterns [10].

By integrating spatial migration vectors and temporal cycle components to construct a spatiotemporal joint coupling transfer matrix, and combining the cross-regional propagation characteristics of lateral pulses from PCNN neurons, the spatiotemporal linkage evolution of hotspots driven by social information propagation is simulated, and the future heat distribution trend at the geographic grid granularity is predicted [11], achieving a closed-loop analysis throughout the entire process. The core spatiotemporal coupling inference model can be expressed by formula (12):

$$\begin{cases} \dfrac{\partial Q}{\partial t} = K_{tm} \cdot Q + K_{st} \cdot \nabla Q \\ Q(t+\Delta t) = \Phi_{prop}\left(Q(t), W_{pcnn}\right) \end{cases} \tag{12}$$

In formula (12), K_{tm} and K_{st} are the temporal evolution coefficient matrix and the spatial diffusion coefficient matrix, respectively; Φ_{prop} is the propagation inference operator; W_{pcnn} is the PCNN lateral synaptic weight matrix; Δt is the inference time step; Q is the global grid spatiotemporal heat field vector.

Based on this model, the distribution of tourism popularity at the geographic grid level within the future time window is inferred, realizing a closed-loop analysis of the entire process from current status identification, pattern deconstruction to trend prediction. Thus, this paper completes the research on the spatiotemporal evolution analysis of social media tourism hotspots based on pulse-coupled neural networks and memristor cross arrays.

5. Experiments

5.1. Experimental Environment and Dataset Configuration

This paper uses a hardware and software co-simulation platform to carry out experiments. The hardware main control end is equipped with a high-performance multi-core CPU and a parallel acceleration GPU. A large-scale TiO_2-based memristor cross array simulation environment is built based on the MemTorch open-source framework to reproduce the array resistance characteristics and in-situ storage and computation functions; the software environment is based on the Python compilation deep learning framework to complete the TS-PCNN network construction, tensor data processing and evolutionary analysis and reasoning.

The experimental dataset selects the annual social media cultural tourism UGC tensor data of the provincial administrative region in Central China. After coordinate correction, duplicate sample removal, noise filtering and invalid component cleaning, the original data generates standardized high-order feature tensors, covering four typical scenarios: mountain natural scenic spots, river and lake waterfront scenic spots, urban cultural tourism business districts and rural leisure cultural tourism. The tensor dimension and sample distribution information of the dataset are shown in Table 3.

Table 3. Dataset Tensor Dimensions and Sample Distribution Information

Cultural and tourism scene category	Effective tensor sample size	Coverage range of spatial dimension	Temporal dimension span
Mountain natural scenic spots	large-scale	Provincial Nature Reserve	Continuous time series throughout the year
River and Lake Waterfront Scenic Area	Medium to large scale	Provincial level water system coverage	Continuous time series throughout the year
Urban cultural and tourism business district	ultra-large-scale	Scope of built-up areas in prefecture level cities	Continuous time series throughout the year
Rural leisure tourism	Small and medium-sized	Cluster scope of rural demonstration sites	Continuous time series throughout the year

5.2. Experimental Results and Analysis

The core spatiotemporal evolution path matching performance is quantitatively evaluated, and the results are shown in Figure 2.

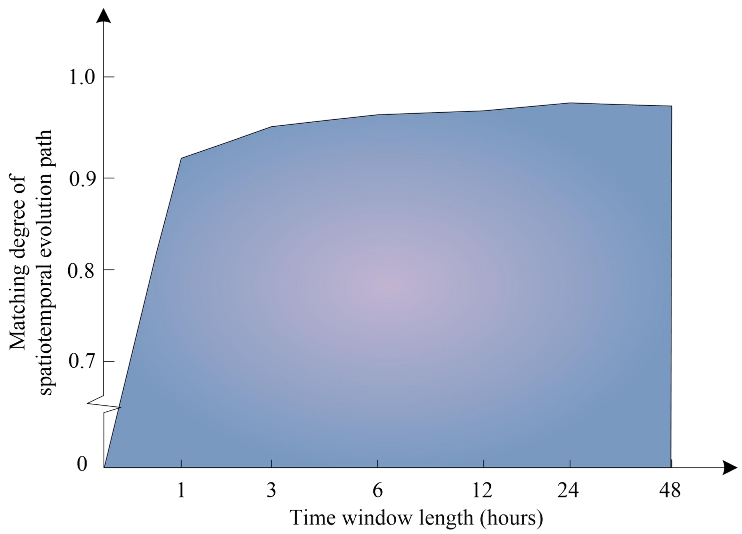

Figure 2. Change curve of spatiotemporal evolution path matching degree of social media tourism hotspots under different time windows

As shown in Figure 2, the spatiotemporal evolution path matching degree changes non-linearly with the length of the time window: the matching degree of the 1-hour short window is only 0.92, the accuracy of the 3-hour, 6-hour, and 12-hour windows gradually increases to 0.97, the 24-hour daily window reaches a peak of 0.975, and the accuracy of the 48-hour long window slightly decreases to 0.972.

This excellent performance stems from the deep collaboration between the hierarchical memristor array and the improved PCNN: isolating and fusing four-dimensional features, accurately capturing UGC fluctuations, mining cross-time period correlations, suppressing long-term time-series noise, adapting to the characteristics of tourism data, and ultimately achieving high-precision path matching.

The accuracy of hotspot identification for four types of cultural tourism scenarios is verified, and the confusion matrix results are shown in Figure 3.

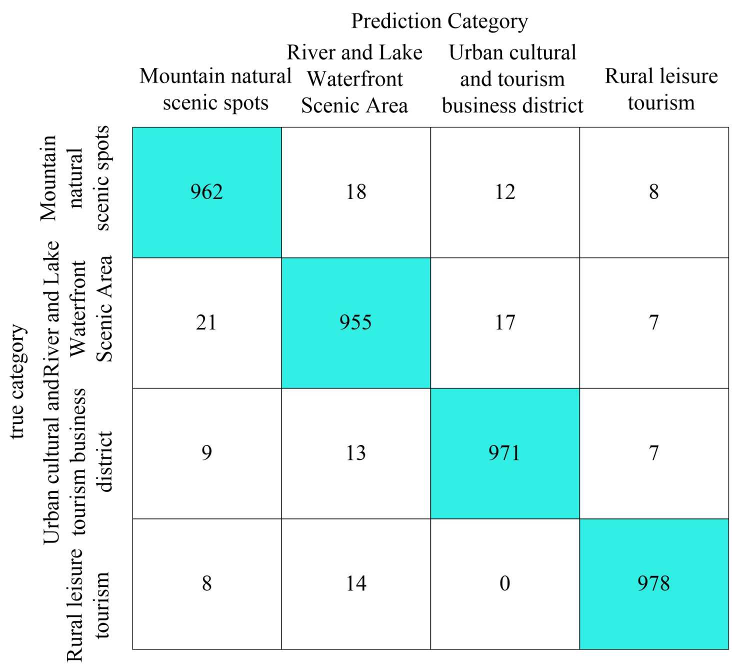

Figure 3. Heatmap of confusion matrix for social media tourism hotspot identification under four types of tourism scenarios

As can be seen from the confusion matrix in Figure 3, the overall classification accuracy of the model in this paper is excellent: 978 rural cultural tourisms are correctly classified, with only a small number of confused samples in the suburbs; 971 urban business districts are correctly classified, with misclassifications concentrated in the overlapping areas of waterfront and rural edges; only 38 and 45 misclassifications are made in mountain and river/lake scenes, respectively, due to the convergence of features between the two types of natural scenes, with no large-scale category confusion, and the model has a very strong scene discrimination ability.

This effect benefits from the hardware and software collaborative architecture: the hierarchical memristor array analyzes four-dimensional features in situ, isolating overlapping interference; the improved PCNN captures scene-specific propagation paradigms through pulse coding, strengthens multimodal differentiated representation, filters latent features, avoids the feature aliasing defects of traditional models, and achieves high-stability and high-precision hotspot recognition in the entire cultural tourism scene.

The method in this paper is set as the experimental group, and the methods mentioned in references [1], [2] and [4] are selected for comparison, respectively set as comparison method 1, comparison method 2 and comparison method 3. The spatiotemporal evolution analysis of social media tourism hotspots is performed using the four methods, and the analysis delay results of the four methods are shown in Table 4.

Table 4. Analysis Delay Results of the Four Methods under Different Input Feature Dimensions

Input feature dimension	Proposed method	Comparison method 1	Comparison method 2	Comparison method 3	Comparison method 4
128	2.1ms	7.3ms	9.5ms	11.2ms	128
512	5.7ms	28.6ms	35.2ms	41.7ms	512
1024	10.3ms	62.1ms	75.4ms	88.3ms	1024
2048	18.7ms	116.2ms	138.5ms	162.4ms	2048

As shown in Table 4, the inference latency of all four methods increases non-linearly with the increase of feature dimension. The increase and absolute time consumption of the proposed method are much lower than those of the control group. At 128, 512, 1024, and 2048 dimensions, the latency of the proposed method is only 2.1ms, 5.7ms, 10.3ms, and 18.7ms, respectively, while the highest latency of the comparative methods at the same dimension is 11.2ms, 41.7ms, 88.3ms, and 162.4ms. At 2048 dimensions, the latency of the comparative methods increases sharply, but the proposed method still maintains a controllable increase. The higher the dimension, the more significant the performance advantage.

6. Conclusion

This paper conducts spatiotemporal evolution analysis of social media tourism hotspots based on pulse-coupled neural networks and memristor cross arrays. Experimental results show that the path matching accuracy reaches 0.975 under the optimal 24-hour time window, with ≥955 correctly classified samples for each of the four types of cultural and tourism scenarios and ≤45 misclassifications across scenarios. The inference latency is only 18.7ms under 2048-dimensional high-dimensional feature input, which is up to 8.7 times faster than traditional models, effectively solving the engineering problems of high latency and low energy efficiency in high-dimensional cultural and tourism data processing.

Funding

This work was supported by the Soft Science Research Program Fund of Henan Province under the project “Research on the Protection and Innovative Path of Red Food Culture in Henan Driven by Tourism” (Grant No. 252400410320), and the 2025 Cultural and Tourism Research Fund Project of Henan Province under the project “Research on the Development of Red Rural Sports Tourism in the Dabie Mountains of Henan Under the Integrated Model of Agriculture, Sports and Tourism” (Grant No. whlv2025080).

Zhuoran Zhang (born October 1982), male, Han Chinese, holds a Ph.D. in Business Administration. He is the Director of the Doctoral Program and a Doctoral Supervisor at the Martin de Tours School of Management and Economics, Assumption University, and concurrently serves as the Director of the Dual Ph.D. Program. His primary research interests include environmental economics, consumer behavior, and tourism development.

References

1. Foka D O G ,Mishra S ,Stanica R , et al. Hotspot analysis and prediction for mobile networking applications [J]. Annals of Telecommunications, 2026, 81 (1-2): 1-16. DOI:10.1007/S12243-026-01144-1
2. Yujuan Z. Travel Best Route Recommendation Algorithm Using Social Networks and Interest Hotspots Map[J].International Journal of e-Collaboration (IJeC),2025,21 (1):1-18.DOI:10.4018/IJEC.369391
3. Liu Y, Qi F ,Du H , et al. County-Level Hotspot Identification and Spatial Regression Analysis of Health Loss from Kashin-Beck Disease - China, 2019 and 2023. [J]. China CDC weekly, 2025, 7 (45): 1418-1423. DOI:10.46234/CCDCW2025.237
4. Dunkel A , Burghardt D , Gugulica M .Generative Text-to-Image Diffusion for Automated Map Production Based on Geosocial Media Data[J].KN - Journal of Cartography and Geographic Information, 2024, 74(1):3-15.DOI:10.1007/s42489-024-00159-9
5. Gu Z, Gao T, Bai Z, et al. Research of Crowd Behavior Simulation Methods Based on Relationships and Emotional Evolution[J]. ACM Transactions on Modeling and Computer Simulation, 2026, 36(2): 1-18. DOI:/10.1145/3787458
6. Species-level phylogenetic diversity analysis reveals a global biodiversity hotspot in Central China [J]. Nature Ecology & Evolution, 2026, 10 (4): 1-2. DOI:10.1038/S41559-026-03033-1
7. Chetia M, Baruah D U. Spatio-Temporal Trends and Hotspot Analysis of Black Carbon over India (1980–2023) [J]. Journal of the Indian Society of Remote Sensing, 2026, 54 (6): 1-16. DOI:10.1007/S12524-025-02405-7
8. Grayon R A, Kahn G L, Trasande L, et al. Environmental Risk and Adverse Perinatal Health Indicators in New York City: A Geospatial Hotspot Analysis [J]. Journal of Urban Health, 2026, 103 (2): 1-12. DOI:10.1007/S11524-026-01060-8
9. Nagihan A C, Eylul D K. Research hotspots, emerging patterns, and intellectual structure of homestay tourism: a bibliometric analysis[J].Quality & Quantity,2023,58 (3):2571-2589.DOI:10.1007/S11135-023-01763-Z
10. Bagheri R, Mohamadi S. Multi-criteria-based hotspot analysis for prioritization of native woody species in sustainable biologic programs for arid lands [J]. Landscape and Ecological Engineering, 2025, 21 (3): 1-18. DOI:10.1007/S11355-025-00654-9
11. Perez A M P , Reynoso R J B , Salangsang S P T ,et al.Dolomite Beach as a Tourist Attraction in Manila as Perceived by Local Residents: Basis for Tourism Promotion[J].International Journal of Marketing and Digital Creative, 2024, 2(1):46-58.DOI:10.31098/ijmadic.v2i1.2243

About the Author

Qian Zhang (born October 1982), female, Han Chinese, native of Jiaozuo, Henan Province. She is currently a Ph.D. candidate at the Martin de Tours School of Management and Economics, Assumption University, and an associate professor at Jiaozuo Normal College. Her primary research interests include leisure tourism and rural tourism.